AtHB40 modulates primary root length and gravitropism involving *CYCLINB* and auxin transporters

Catia Celeste Mora [a], María Florencia Perotti [a], Eduardo González-Grandío [b], Pamela Anahí Ribone [a], Pilar Cubas [b], Raquel Lía Chan [a,*]

[a] *Instituto de Agrobiotecnología del Litoral (CONICET, Universidad Nacional del Litoral, FBCB), Colectora Ruta Nacional 168, km 0, 3000 Santa Fe, Argentina*
[b] *Centro Nacional de Biotecnología (CNB) - CSIC, Madrid, Spain*

ARTICLE INFO

Keywords:
AtHB40
HD-Zip
LAX2
LAX3
PIN2
CYCLINB1.1
Gravitropism
Root development

ABSTRACT

Gravitropism is a finely regulated tropistic response based on the plant perception of directional cues. Such perception allows them to direct shoot growth upwards, above ground, and root growth downwards, into the soil, anchoring the plant to acquire water and nutrients. Gravity sensing occurs in specialized cells and depends on auxin distribution, regulated by influx/efflux carriers. Here we report that *AtHB40*, encoding a transcription factor of the homeodomain-leucine zipper I family, was expressed in the columella and the root tip. *Athb40* mutants exhibited longer primary roots. Enhanced primary root elongation was in agreement with a higher number of cells in the transition zone and the induction of *CYCLINB* transcript levels. Moreover, *athb40* mutants and *AtHB40* overexpressors displayed enhanced and delayed gravitropistic responses, respectively. These phenotypes were associated with altered auxin distribution and deregulated expression of the auxin transporters *LAX2*, *LAX3*, and *PIN2*. Accordingly, *lax2* and *lax3* mutants also showed an altered gravitropistic response, and *LAX3* was identified as a direct target of AtHB40. Furthermore, AtHB40 is induced by AtHB53 when the latter is upregulated by auxin. Altogether, these results indicate that AtHB40 modulates cell division and auxin distribution in the root tip thus altering primary root length and gravitropism.

1. Introduction

Root development depends on the surrounding soil composition, severely influenced by climate fluctuations, particularly by frequent drought periods. Salt concentration increases in soils after water deficit episodes, which causes losses of arable land worldwide (Wicke et al., 2011). Roots adapt to the environmental conditions by changing their patterns of growth and development (*i.e.*, primary root growth, lateral root initiation and emergence, gravitropism, halotropism). Gravitropism is a tropistic response based on the perception of directional cues that allows plants to direct growth: shoot upwards and root towards gravity (Vandenbrink and Kiss, 2019). Shoot growth is necessary for photosynthesis, gas exchange, and reproduction, whereas root growth is needed to anchor the plant and acquire water and nutrients. When plants are reoriented relative to gravity, they respond by curving their stems and roots. Among a plethora of environmental cues, plant roots perceive gravity and direct development in a response called gravitropism which can be divided into three phases, perception, signal transmission, and growth (Swarup and Bennett, 2009). These phases are temporally and spatially separated and take place by characterizing specialized cells. Gravity is perceived in the columella cells, as demonstrated by several elegant ablation experiments, and gravitropism takes place in the elongation zone after signal transduction (reviewed by Sato et al., 2015; Vandenbrink and Kiss, 2019). Columella cells contain dense starch-filled amyloplasts able to change their localization in the cells and redirect auxin from the sensing site (the root cap statocyte) to the response location in the elongation zone (reviewed by Su et al., 2017; Su and Masson, 2019). Plant adaptation to the environment depends on this process.

Regarding the role of auxin in root gravitropism, auxin efflux/influx carriers (*i.e.* PINFORMED and AUX/LAX, respectively) create a hormone gradient between the upper and lower regions of the root (Rakusová et al., 2015; Zhang et al., 2019).

Transcription factors (TFs) are crucial players in gravitropism that

Abbreviations: HD-Zip, homeodomain-leucine zipper; TF, transcription factor; WT, wild type; GUS, β-Glucuronidase.

* Corresponding author.
E-mail address: rchan@fbcb.unl.edu.ar (R.L. Chan).

modulate the expression of genes encoding auxin transporters and proteins involved in amyloplast synthesis (Motte et al., 2019). Such regulation, as in other developmental events, occurs, directly or indirectly, through other biomolecules acting as intermediates (Gonzalez, 2016). The homeodomain-leucine zipper TF family (HD-Zip), which comprises clades I–IV (Capella et al., 2016), includes several gene members expressed in specific root cell types, but their roles in root development and gravitropism are only partially known (Perotti et al., 2021). Only a few Arabidopsis members were assigned functions in root development. The paralogs AtHB7 and 12 were associated with aluminum stress response (Liu et al., 2020). *AtHB13* was assigned a role as a negative regulator of early root growth (Silva et al., 2016). Its paralog, *AtHB23* directly regulated *LAX3* and *LBD16*, leading to an increased number of initiated lateral roots in *amiR23*-silenced plants (Perotti et al., 2019, 2020). AtHB52 plays a role in the crosstalk between auxin and ethylene (Miao et al., 2018). Moreover, *AtHB52* mutants and overexpressors showed distorted auxin distribution and gravitropism and directly regulate the expression of *PIN2* involved in auxin transport (Miao et al., 2018). AtHB53 was also linked to auxin/cytokinin signaling pathways in roots (Son et al., 2005), and AtHB40 was proposed as a direct regulator of *LAX3*, based on a yeast one-hybrid approach (Porco et al., 2016).

Arabidopsis *AtHB21*, *AtHB40*, and *AtHB53* are paralog genes of the clade VI of HD-Zip I TFs (Arce et al., 2011). *AtHB40*, evaluated by non-quantitative RT-PCR, was detected in flowers and siliques and regulated by ABA and NaCl in seedlings, and *AtHB53* was expressed in roots, induced by auxin and repressed by cytokinin (Henriksson et al., 2005), but no functional characterization of these genes was carried out so far (Son et al., 2005). The role of *AtHB21* remains largely unknown. Recently, it was reported that its homolog in tung tree (*VtHB1*) is strongly expressed in densely shaded seeds during the rapid oil accumulation period (Zhang et al., 2021). Regarding the aerial organs, it was reported recently that these three genes are induced by BRC1, and these TFs act redundantly as positive regulators of *NCED3* together with BRC1, a master regulator of axillary bud growth and are required for axillary bud suppression in shade (Gonza´lez-Grandío et al., 2017). Also in aerial organs, AtHB40 was identified as a modulator of the *JUNGBRUNNEN1 - GA 2-OXIDASE* regulatory module for gibberellin homeostasis (Dong et al., 2022).

In this work, we report the functional characterization of *AtHB40* in roots. Using mutant and constitutive and inducible overexpressor lines, we show that this TF acts as a negative regulator of primary root growth and the gravitropistic response. *ATHB40* is induced by auxin in the root tip and root vasculature. Moreover, it represses the *CYCLINB1.1* gene in the transition zone of the root as well as genes encoding the auxin transporters LAX2, and LAX3 in the root tip and vasculature, and PIN2 in the lateral root cap. Among them, *LAX3* seems to be a direct target of AtHB40, whereas the others require other unidentified intermediates. Notably, the modulation of gravitropism in plants with altered *AtHB40* levels occurs via auxin distribution in the root tip and does not affect amyloplasts formation.

2. Materials and methods

2.1. Plant material, growth conditions, transformation, and crosses

Seeds of *Arabidopsis thaliana* (Col-0 ecotype), mutant, and overexpressor plants, were surface sterilized and placed at 1 cm from the top of square Petri dishes (12 × 12 cm) for 3 days at 4 °C before placing the dishes in the growth chamber at 22–24 °C under long-day (16/8 light/dark cycles) with a light intensity of approximately 70 μmol m^{-2} s^{-1}. The growing medium was Murashige-Skoog supplemented with vitamins (MS, PhytoTechnology Laboratories™.

For roots surveys, photograph series were taken and analyzed with ImageJ and RootNav free software.

Stable transformations of Arabidopsis plants were performed via a floral dip procedure as previously described (Clough and Bent, 1998). *Agrobacterium tumefaciens* strain, LBA4404, carrying the constructs described below, was used to transform. The selection was performed on the basis of their resistance to the appropriate selector chemical (Basta 50 mg/l or kanamycin 50 mg/l).

Transgene insertions were verified by PCR using genomic DNA as a template and specific oligonucleotides (Table S1). Three/four positive independent lines were further reproduced and homozygous T3 and T4 plants were used to further tests.

Transgenic plants transformed with $AT40_{ind}$, *HB40p:GUSt*, *HB53p:GUS*, *HB21p:GUS* constructs were previously obtained and described (Gonza´lez-Grandío et al., 2017).

Transgenic plants carrying *AUX/LAX* promoters fused to *GUS*, previously described (*prAUX1:GUS*: Marchant et al. 1999, 2002; *prLAX1:GUS*: Bainbridge et al. 2008 and *prLAX3:GUS*: Swarup et al. 2008), were generously gifted by Dr. Swarup' lab. *DR5:GFP* transgenic plants, as well as *athb40* mutant lines (*athb40*-1, *athb40*-2, and *athb40*-3) were obtained from ABRC (Arabidopsis Biological Resource Center).

2.2. Plant crosses

Mutant plants *athb40–1*, *athb40–2*, and *athb40–3* were fertilized with pollen from *prCYCLINB:GUS*, *prAUX1:GUS*, *prLAX2:GUS*, *prLAX3:GUS*, *prPIN2:YFP* and *DR5:YFP* genotypes, and then selected by the corresponding selector chemical, depending on the donor (kanamycin resistance for the constructs bearing the promoters of *LAX2*, *LAX3*, and *AUX*, and BASTA for the one bearing the *PIN* promoter). The same procedure was followed to obtain the crosses between *athb40* and *athb53* mutants with *prAtHB53:GUS* and *prAtHB40:GUS* plants.

2.3. Genetic constructs

prAtHB40:GUS: a 1995 bp DNA segment upstream of the + 1 of *AtHB40* cDNA was amplified by PCR using the primers detailed in Supplementary Table S1 and genomic DNA from *Arabidopsis thaliana*. The PCR product was then cloned in the *pENTR D-Topo* and then recombined by the Gateway® system (Invitrogen) with the *pK2GWFS7* vector.

35S:AtHB40: the *AtHB40* cDNA was amplified by PCR using RNA extracted from flowers and the oligonucleotides listed in Supplementary Table S1. The amplicon was cloned in the *pGEMT-easy* vector and then restricted with *Sac*I and *Kpn*I and subcloned in the same sites of the *pBI122* vector.

2.4. GUS histochemistry

In situ assays of GUS activity were performed essentially as described by Jefferson et al. (1987) with little modifications (Ribone et al., 2015).

2.5. Fluorescence microscopy

For confocal imaging, seedlings roots from different genotypes, including *athb40* and AT40 mutants, were treated with 10 μg/ml propidium iodide, rinsed with a drop of distilled water, and examined and imaged using a confocal inverted microscope (Confocal LEICA TCS SP8). The observations were done using a 20 × objective, a 514 nm excitation line laser for propidium iodide (18 % intensity) and YFP (50 % intensity), and appropriate emission at 498 nm, — 532 nm, 523 nm, and — 594 nm bandpass filters, respectively. When the samples analyzed were the crosses with *DR5:GFP* and *prPIN2:YFP* the propidium iodide staining was omitted and the followed procedure was the same as described above.

2.6. Gravitropism assays

For root gravitropism assays, seeds were germinated on MS medium

plates and grown vertically for seven days under long-day conditions under a 16-h light/8-h dark cycle. Plates were then rotated 90°. After 6 h of the gravitational stimulus, plates were photographed and images were used for the determination of root reorientation, employing the angle tool of ImageJ. The root tip angle of individual roots at time point zero was defined as 180° according to Muller et al. (2018).

2.7. Amyloplasts staining and light microscopy observation

To observe the amyloplasts in the columella cells of the root tips, 15–20 Arabidopsis roots (5 day-old) were dipped in Lugol staining solution (Sigma-Aldrich) for 3–5 min, washed with distilled water, and then observed in an Eclipse E200 Microscope (Nikon, Tokyo, Japan, https://www.nikon.com/) equipped with a Nikon Coolpix L810 camera.

2.8. RNA isolation and analysis

Total RNA used in qRT-PCR was isolated from Arabidopsis roots using Trizol® reagent (Invitrogen) according to the manufacturer's instructions. One μg of RNA was reverse-transcribed using oligo(dT)18 and M-MLV reverse transcriptase II (Promega). Quantitative real-time PCR (qPCR) was performed using a StepOnePlus Real-Time Systems (Applied Biosystems TM); Each reaction contained 10 μl final volume having 5 μl Taq TM SYBR® Green Supermix, 0,2 μl of each specific oligonucleotide (10 pmol/μl; Supplementary Table S1) and 1/20 of RT product. Fluorescence was measured at 72 °C during 40 cycles. Quantification of mRNA levels was achieved by normalization against *ACTIN* transcripts levels (*ACTIN2* and *ACTIN8*) following the ΔΔCt method. All of the reactions were performed with at least three biological replicates and bars represent SEM.

2.9. Chromatin immunoprecipitation followed by quantitative PCR (ChIP-qPCR)

For ChIP-qPCR assays, 10-day-old seedlings bearing the construct *LexA:minimal35S:HA:HB40* were harvested and nuclei prepared as described in Lucero et al. (2017). For the IPs, protein A Dynabeads (Thermo) and anti-HA ab9110 antibodies (Abcam) were used. In both ChIP-qPCR experiments, the anti-IgG ab6702 antibody (Abcam) was used as a negative control. Chromatin was sheared using the Picoruptor sonicator (Diagenode; 10 cycles 30" ON, 30" OFF). PCR with specific oligonucleotides (see Supplementary Table S1) was performed using the Sso Advanced Universal mix (BioRad) in a StepOne device (Applied Biosystems).

2.10. Statistical analysis

Error bars in the graphics showing the evaluation of primary root length, density of initiated and emerged secondary roots, and root tip angles represent SEM. Asterisks indicate significant differences doing a Student's t-test between Col 0 and each transgenic line (*$P < 0.05$, ** $P < 0.01$, *** $P < 0.001$, **** $P < 0.0001$) or doing an ANOVA test between Col 0 and each transgenic line (** $P < 0.01$, *** $P < 0.001$, **** $P < 0.0001$). The number of biological replicates for each assessment is indicated in the corresponding figures.

2.11. Accession numbers

AT4G36740 (AtHB40); AT5G66700 (AtHB53); AT2G18550 (AtHB21); AT4G37490 (CYCLINB); AT2G38120 (AUX1); AT2G21050 (LAX2); AT1G77690 (LAX3); AT5G57090 (PIN2).

3. Results

3.1. AtHB40 expression is localized at the primary and lateral root tips

AtHB40 transcripts were detected in 12-day-old roots by non-quantitative RT-PCR (Henriksson et al., 2005), but no detailed expression patterns were available so far. According to the information at the BAR and Root Atlas repositories (Brady et al., 2007; Dinneny et al., 2008; Kilian et al., 2007; Zhang et al., 2019), the mRNA of this gene was detected in the lateral root cap, the phloem-pole-pericycle, the phloem companion cells, and the stem-cell niche. However, plants transformed with a 1000 bp genomic region upstream of the + 1 driving the expression of the *GUS* reporter gene did not show any expression in roots (Gonza´lez-Grandío et al., 2017), suggesting that some regulatory motifs were lacking. Therefore, we made a new construct with a 2 kb genomic segment upstream of the + 1 driving the expression of the *GUS* reporter gene. Several independent transgenic lines carrying this construct were obtained and analyzed by histochemistry (Fig. 1 and Supplementary Fig. S1). GUS activity was specifically localized in columella cells and, at lower levels, in the vascular system of the primary root and lateral roots (LR) and the tip of LR (Fig. 1). The expression was weak in 3-day-old seedlings and increased steadily until 15 days after sowing (Fig. 1 A). This observation indicated that the genomic region comprised between — 1000 and — 2000 was necessary for expression in roots. Besides, the expression was detected in axillary buds, shoot, the apical meristem, and in a generalized manner in young developing flowers in agreement with previous reports (Supplementary Fig. S2). In contrast, neither *AtHB53* nor *AtHB21* was expressed in columella cells; *AtHB53* showed specific expression in lateral roots (Supplementary Fig. S3; Gonzalez-Grandío et al., 2017), and *AtHB21* activity was not detectable at all, suggesting that each member of this HD-Zip I clade has acquired specific functions in roots during evolution.

3.2. AtHB40 is a repressor of primary root growth at the transition zone

To investigate the role of AtHB40 in roots, three independent homozygous mutant lines (named *athb40-1*, *athb40-2*, and *athb40-3*) were obtained (Fig. 2a). *AtHB40* transcripts were not detectable in any of these alleles. Primary roots were significantly longer in 6-day-old mutants than in their wild-type counterparts (Fig. 2b). This difference was associated with an increase in cell number at the transition zone in two out of the three mutant lines, as observed by confocal microscopy after root staining with propidium iodide (Figs. 2c and 2d). In accordance, overexpressor plants exhibited the opposite phenotype. We obtained both estradiol-inducible (*LEXA:AtHB40*, thereafter $AT40_{ind}$), and constitutive (*35S:AtHB40*, named AT40) *AtHB40* overexpressors. The expression levels of AT40 (5–20 fold over the WT) and $AT40_{ind}$ (580 fold after 6 h induction) lines are shown in Supplementary Fig. S4a. AT40 plants had shorter roots (Fig. 2g), whereas $AT40_{ind}$ lines showed the same phenotype after estradiol treatment (Fig. 2e). Moreover, $AT40_{ind}$ plants exhibited a curved root shape which suggested alterations in gravity sensing (Fig. 2f), while AT40 lines exhibiting very high expression levels lead to aberrant or lethal phenotypes (Supplementary Fig. S4b). These results indicate that AtHB40 may be a repressor of the primary root elongation and is also involved in gravitropism.

In contrast, AtHB40 does not seem to play a key role in LR development, at least in normal conditions; mutant and WT genotypes showed a similar number of total lateral roots, although the mutant genotype exhibited slightly fewer initiated roots (Supplementary Fig. S5).

3.3. AtHB40 modulates the expression of CYCLINB1.1

Aiming at understanding the molecular mechanism underlying AtHB40 function in root elongation, *athb40* mutants, AT40, and AT40ind plants were crossed with plants transformed with the promoter

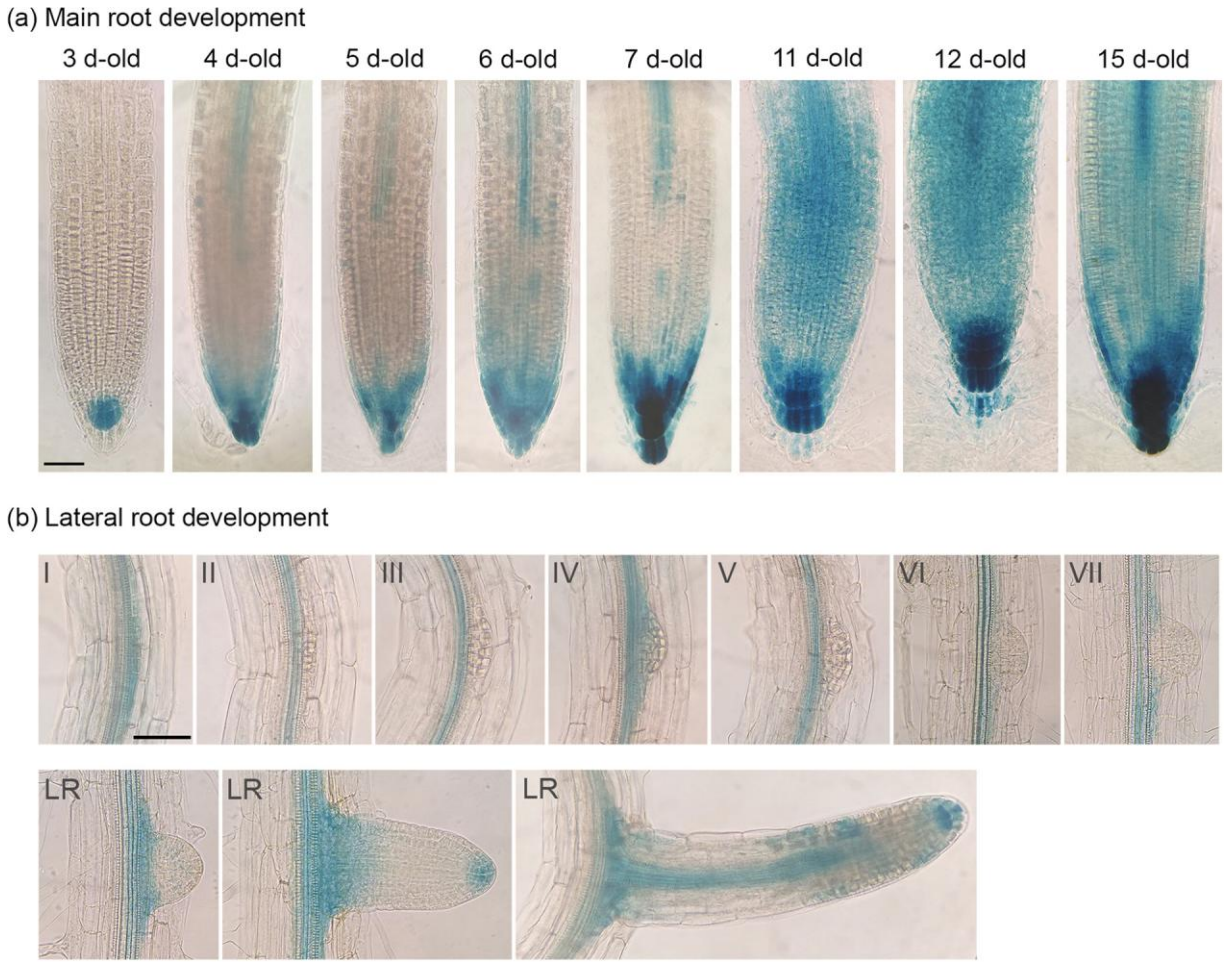

Fig. 1. ***AtHB40 is expressed in the tip of the main and lateral roots.*** Illustrative pictures showing GUS expression driven by *AtHB40* promoter (*prAtHB40:GUS* plants) in the main **(a)** and in lateral roots of 7-day-old seedlings (**b**). (**a**) Kinetics of *AtHB40* expression in the primary root during growing in Petri dishes in normal conditions, starting at 3 days until day 15. (**b**) Different developmental stages of lateral root development. The assays were repeated at least three times with N: 15. Black bars represent 40 μm.

of *CYCLINB1.1* driving the expression of the β-glucuronidase (GUS) reporter gene (*prCYCLINB1.1:GUS*). Crossed lines were analyzed by histochemistry. Those of *athb40*, AT40, and AT40ind combined with *prCYCLINB1.1:GUS* exhibited a clear increase and decrease of GUS staining, respectively (Fig. 3a). This result suggested that in 7-day old seedlings, AtHB40 represses *CYCLINB1.1* expression, and this is probably the reason for the primary root length differential phenotype observed in the mutant and overexpressor plants. Next, transcript levels of *CYCLINB1.1* were evaluated in whole roots of overexpressor plants (AT40 and $AT40_{ind}$) and *athb40* by qPCR. *CYCLINB1.1* was down-regulated in AT40 and $AT40_{ind}$, whereas no significant differences were observed in the mutants (Fig. 3b). The lack of significant differences in transcript levels in *athb40* could be due to the dilution of the signal when sampling the whole root.

3.4. AtHB40 plays a key role in root gravitropism

To investigate whether AtHB40 plays a role in root gravitropism, we tested 7-day-old *athb40* mutant and AT40 overexpressor plants grown in vertical plates. Such plates were turned 90° clockwise and after 6 h, angles formed by the root tip were measured (Fig. 4a–c). It is important to note that smaller angles indicate faster responses, whereas the opposite occurs when larger angles are measured (Muller et al., 2018). All the mutant lines showed a significantly smaller angle than controls (Fig. 4b), indicating an enhanced response to gravitropism. In contrast, AT40 plants exhibited larger angles (Fig. 4c), suggesting that AtHB40 is a negative regulator of the gravitropic response.

One of the events usually concomitant with alterations in gravitropism is amyloplast damage (Nakayama et al., 2012). Thus, amyloplasts of mutant, AT40, and control plants were observed after staining with Lugol solution but no significant differences were observed between mutants and controls (Fig. 4d), indicating that the altered gravitropistic response occurs through a different pathway.

3.5. AtHB40 disturbs auxin distribution in the root tip

To understand the altered gravitropic response of *athb40* and AT40 plants and considering the link between gravitropism and auxin, we studied whether *AtHB40* could affect the expression of auxin influx carriers. For this, *athb40* plants were crossed with *prAUX1:GUS*, *prLAX1:GUS*, *prLAX2:GUS*, *prLAX3:GUS*, and *PIN2:YFP* reporter lines. Seven-day-old *athb40* x *prLAX3:GUS* seedlings exhibited a stronger GUS staining in the columella cells than *prLAX3:GUS* seedlings (Fig. 5a). Moreover, transcript levels of *GUS* were quantified in these crossed plants showing the same result; in other words, upregulation of the target in the mutant compared with *prLAX3:GUS* plants (Supplementary Fig. S6). Likewise, *athb40* × *prLAX2:GUS* crossed seedlings showed stronger GUS activity than *prLAX2:GUS* plants, both in the tip and the vasculature (Fig. 5b) and *athb40* × *PIN2:YFP* plants displayed enhanced fluorescence as compared to *PIN2:YFP* seedlings (Fig. 5c). This indicated that AtHB40 repressed the expression of these auxin carriers somewhere in the signal transduction pathway/s modulated by this TF. In contrast,

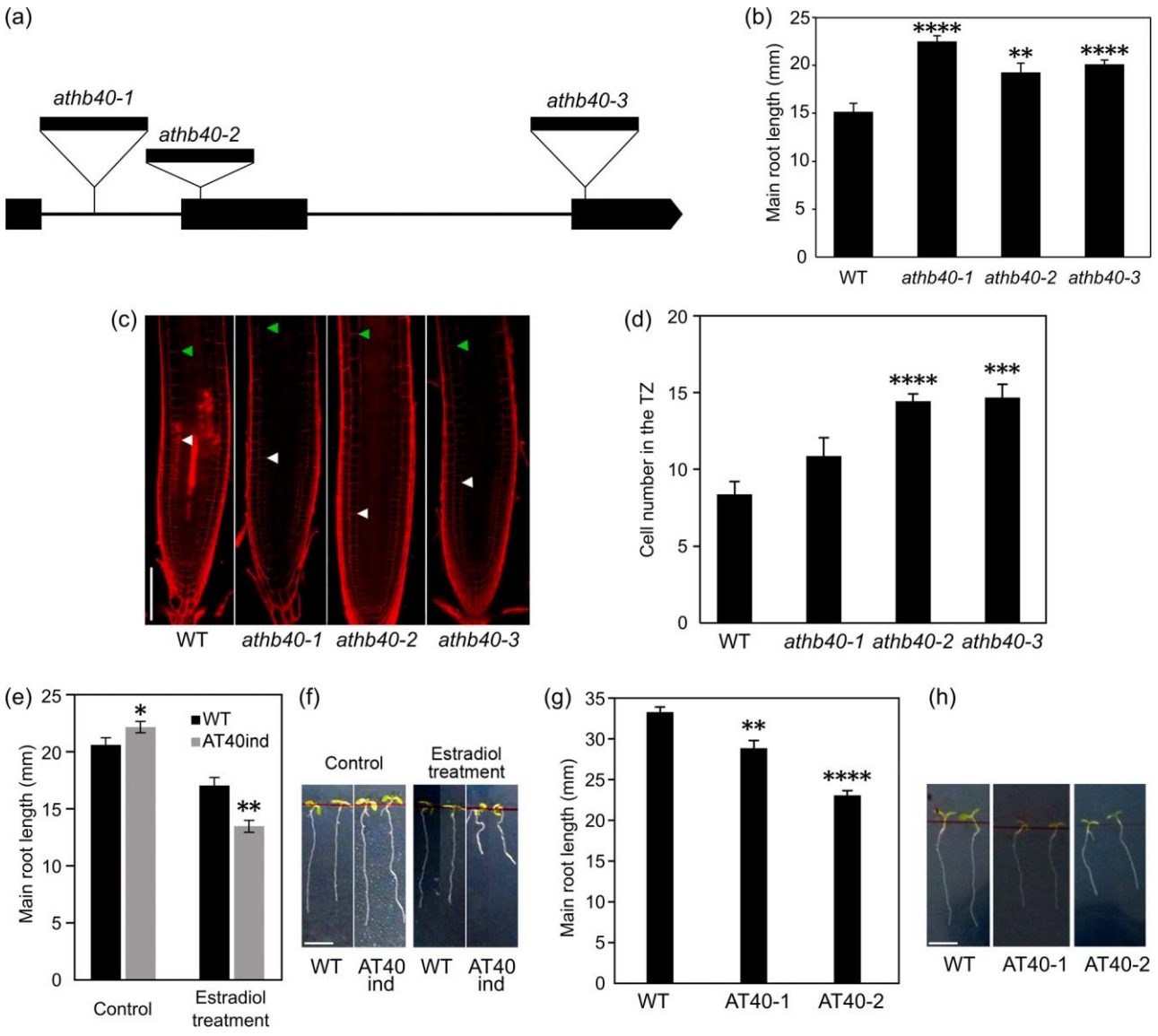

Fig. 2. AtHB40 is a repressor of root elongation. Schematic representation of three *athb40* insertional mutants (*athb40-1*, *athb40-2*, *athb40-3*); filled boxes are exons and lines, introns, whereas, arrowheads indicate the locations of the T-DNA insertions for each mutant. **(b)** Primary root length of 6-day-old Col 0 (WT), *athb40-1*, *athb40-2*, and *athb40-3* plants. **(c)** Illustrative picture of Col 0 (WT), *athb40-1*, *athb40-2*, and *athb40-3* plants taken with the confocal microscope after staining with propidium iodide. Arrows indicate the beginning and the end of the transition zone (TZ). The white bar represents 100 μm. **(d)** The number of cells in the TZ. **(e)** Primary root length of 8-day-old Col 0 (WT), and $AT40_{ind}$ plants in standard growth conditions (left), or after elicitation with estradiol (right). **(f)** Illustrative pictures of the same plants as in **(e).** (**g**) Primary root length of 8-day-old Col 0 (WT), and constitutive AT40 plants (two independent lines AT40-1 and AT40-2), and (**h**) illustrative pictures of same the plants as in (**g**). White bars represent 5 mm. The assays were repeated at least three times with N: 15/genotype. Error bars represent SEM. Asterisks indicate significant differences doing a Student's t-test between Col 0 and each transgenic line (*P < 0.05, ** P < 0.01, *** P < 0.001, **** P < 0.0001).

prAUX1:GUS and *prLAX1:GUS* did not respond to changes in *ATHB40* levels (Supplementary Fig. S7).

Furthermore, transcript levels of *LAX2*, *LAX3*, and *PIN2* were measured in *athb40* plants, where a significant induction of *LAX2* and *PIN2* was detected relative to WT (Figs. 5e and 5f). On the other hand, *LAX3* transcript levels did not show differences between mutants and controls (Fig. 5g), probably because the induction is visualized only in a few columella cells, whereas the expression is detected in the whole vascular root system (Fig. 5a) provoking the signal dilution. Regarding *PIN2* modulation by AtHB40, and that *PIN3*, *PIN4*, and *PIN7* also play a role in gravitropism, expression levels of the encoding genes were also quantified. None of them showed up or down-regulation in such mutants (Supplementary Fig. S8). However, it cannot be ruled out that, since the expression of *AtHB40* is localized in a few columella cells, the extraction of total RNA from whole roots masked induction/repression signals. In agreement with this possibility, a transcriptome analysis carried out comparing 7-day-old *athb40* and WT roots revealed only 68 differentially expressed genes (Supplementary Table S1). Among them, a few related to abiotic and biotic stresses and several encoding TFs were modulated. However, we were not able to detect an enriched network or signal transduction pathway. Moreover, none of the auxin carriers analyzed here was in this shortlist (Supplementary Table S2).

These results led us to further investigate auxin distribution/response in the *athb40* and AT40 root tips by crossing these plants with those carrying the auxin response reporter *DR5:GFP*. Although *athb40* mutants did not show alterations in *DR5:GFP*, AT40, displayed a significantly diminished GFP signal, suggesting that *ATHB40* represses auxin transport to the root tip (Fig. 5d).

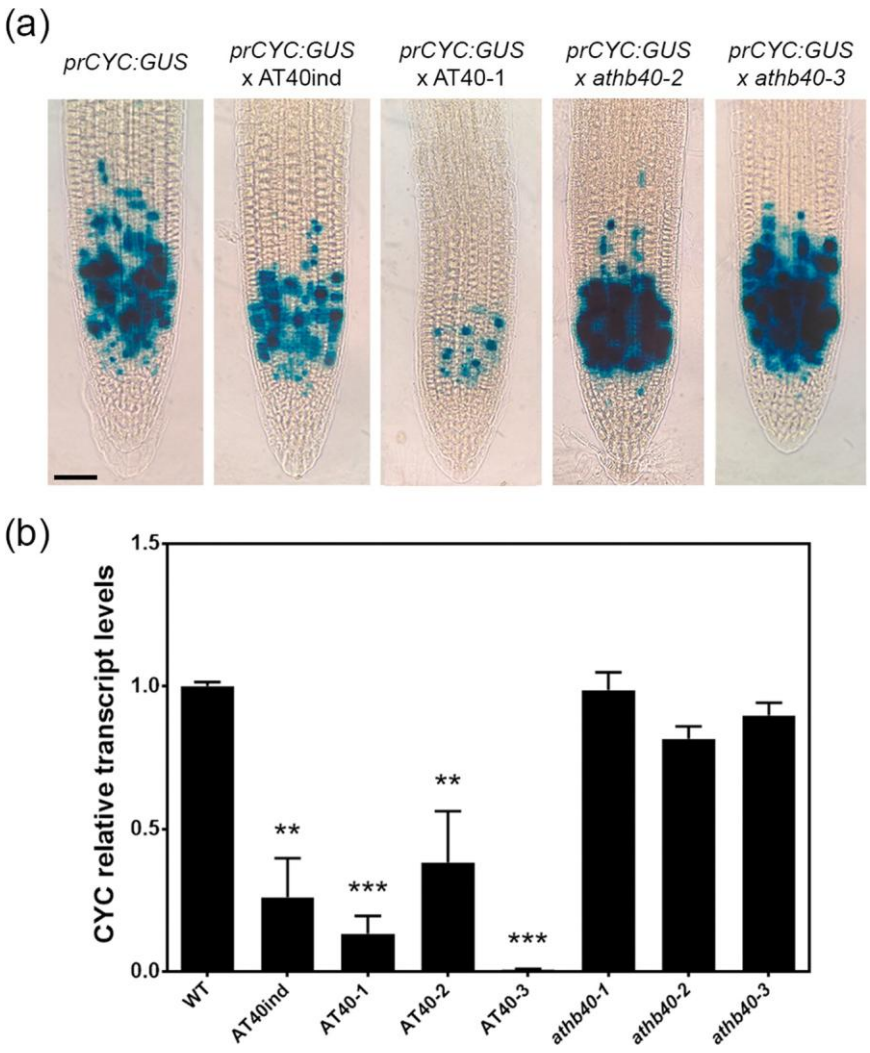

Fig. 3. *CYCLINB* expression is modulated by AtHB40. Illustrative pictures of 7-day-old *prCYCLINB:GUS*, $AT40_{ind}$× *prCYCLINB:GUS*, AT40-1 × *prCYCLINB:GUS*, and *athb40* × *prCYCLINB:GUS* (*athb40-2* and *athb40-3*) roots after histochemical staining. The black bar represents 40 μm, Transcript levels of *CYCLINB* in 7-day-old AT40 overexpressor lines ($AT40_{ind}$, AT40-1, -2, and -3) and *athb40* mutants, compared with the control Col 0, grown in standard conditions. All the values were normalized with the one obtained in Col 0, and represent biological triplicates. Error bars represent SEM. Asterisks indicate significant differences doing an ANOVA test between Col 0 and each transgenic line (** $P < 0.01$, *** $P < 0.001$, **** $P < 0.0001$).

Altogether, these results suggested that AtHB40 modulates auxin distribution through the regulation of its transporters, which in turn affects the gravitropistic response.

3.6. AtHB40 alters the gravitropic response through the auxin carriers LAX2, LAX3, and PIN2

We investigated whether the regulated genes were direct targets of AtHB40. The promoters of *CYCLINB1.1*, *LAX2*, *LAX3*, and *PIN2* were analyzed for the presence of target sequences of HD-Zip I TFs (Palena et al., 1999; Johannesson et al., 2001). Among them, only *LAX3* presented one perfect binding motif, the pseudopalindrome CAAT(A/T)ATTG. In addition, both *LAX3* and *CYCLINB1.1* exhibited an imperfect pseudopalindrome binding motif (8 out of 9 bases match with the target, Fig. 6a, and Supplementary Fig. S9) in their promoters. *LAX2* and *PIN2* did not have putative binding sites in their regulatory regions, suggesting that these genes are not direct targets of AtHB40 and other intermediate proteins are necessary for the observed regulation.

To further test whether AtHB40 directly binds *CYCLINB1.1* and *LAX3* promoters, we conducted chromatin immunoprecipitation assays followed by qPCR (ChIP-qPCR) using 10-day-old $AT40_{ind}$ seedlings, in which AtHB40 has a HA tag. Then, we assessed the direct binding of AtHB40 to the promoters of *LAX3* and *CYCLINB1.1*. AtHB40 bound the *LAX3* promoter whereas it did not bind the *CYCLINB1.1* promoter (Fig. 6a and Supplementary Fig. S9). We analyzed in more detail the promoter region of *LAX3* and found that AtHB40 specifically bound both the perfect and imperfect putative binding motifs (— 135 bp, P3, and — 530 bp P2). Other regions (P1 and P4) were not bound by AtHB40 (Fig. 6b). Altogether these results indicated that AtHB40 can directly regulate *LAX3* but not *CYCLINB1.1*. The regulation of the latter might occur by a pathway involving downstream TFs.

In agreement with these results, DAP-Seq analyses (carried out with *in vitro*-obtained TFs and free-chromatin genomic DNA) indicated that AtHB40 can bind the *LAX3* promoter but not the *CYCLINB1.1* promoter (Bartlett et al., 2017).

If the enhanced gravitropistic response of *athb40* mutants was due to increased levels/activity of *LAX2* and *LAX3*, the model predicts that *lax2* and *lax3* mutants would have a reduced gravitropistic response. Indeed, root gravitropism was evaluated in *lax2* and *lax3* mutants and we confirmed that both *lax2* and *lax3* mutants exhibited a slight but significant delay in the gravitropistic response (Fig. 6c). These observations strongly suggest that the altered root gravitropism displayed by the *AtHB40* mutant and overexpressor lines occurs, at least in part, via the regulation of these auxin carriers.

3.7. AtHB40 expression and subsequent role in the root tip could be modulated by its paralog AtHB53

To investigate further the altered gravitropistic response of *athb40* and AT40 plants, we studied whether *AtHB40* responded to auxin. For this, 7-day-old *prAtHB40:GUS* seedlings were treated with IAA (1 μM). We observed that GUS was induced relative to untreated plants, mostly

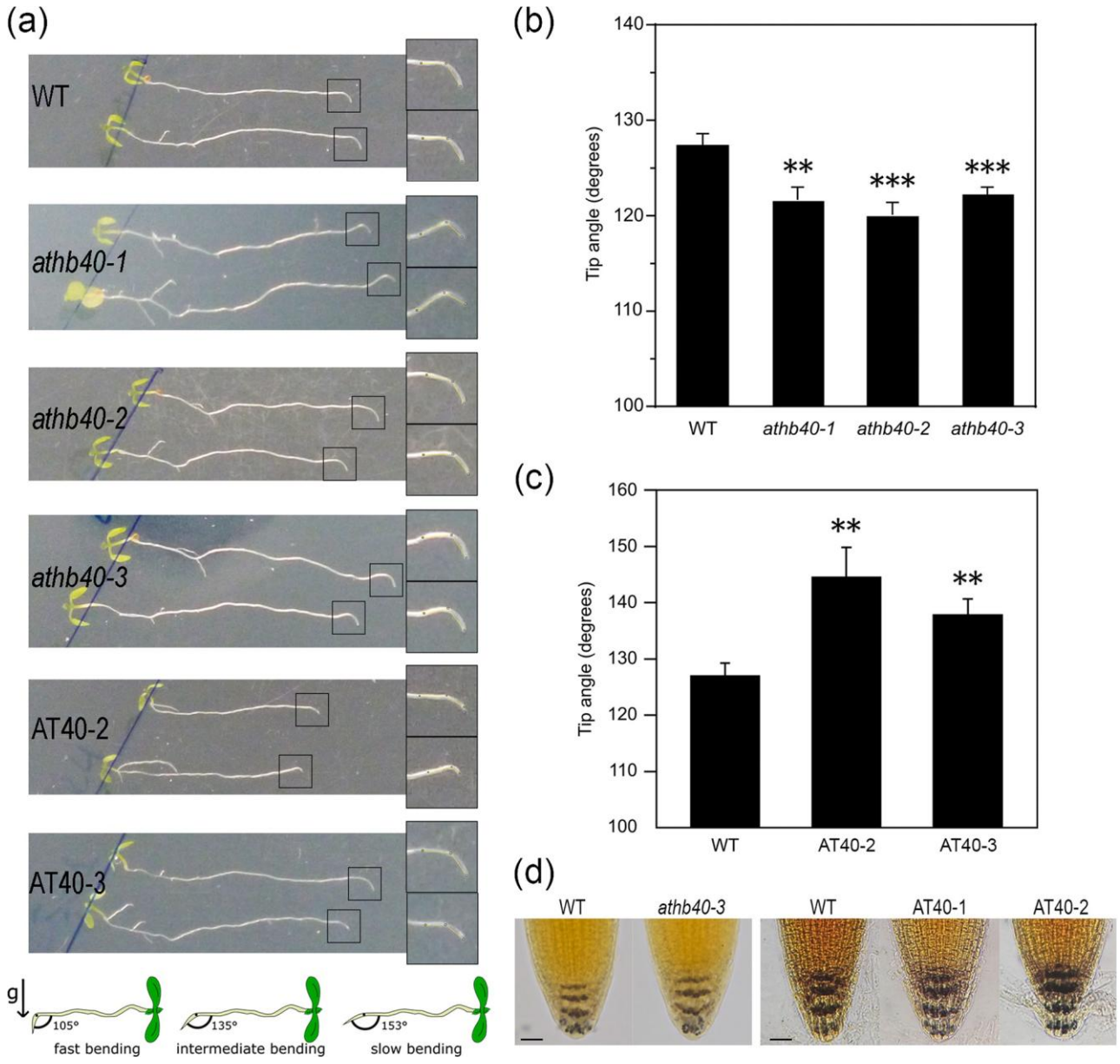

Fig. 4. AtHB40 is a negative regulator of gravitropism. Illustrative pictures of WT, *athb40* (lines *athb40*-1, *athb40*-2, and *athb40*-3), and AT40 (lines AT40-2 and AT40-3) seedlings, showing altered gravitropism. Inset on the right: amplification of the root tip. Black bars represent 100 μm. Bottom: schematic representation of the measured angles. **(b)** The angle was measured in WT, *athb40*-1, *athb*40-2, and *athb*40-3 genotypes, 6 h after turning the plate 90°. **(c)** The angle measured in AT40-2, and AT40-3 overexpressor lines compared with that of control Col 0. (**d**) Illustrative pictures of root tips (5-day-old) stained with Lugol of Col 0, *athb*40-3 mutant seedlings (left), and AT40 (right) grown in normal conditions. The bar represents 30 μm. Error bars represent SEM. Asterisks indicate significant differences doing a Student's t-test between Col 0 and each mutant line (*P < 0.05, ** P < 0.01, *** P < 0.001, **** P < 0.0001).

in the root tip but also in the vascular tissue (Fig. 7a).

Next, we studied the putative relationship of *AtHB40* with *AtHB53*, one of its close paralogs in the root. For this purpose, we generated *athb40* × *prAtHB53:GUS* and *athb53* × *prAtHB40:GUS* lines and analyzed their GUS expression in roots (Fig. 7b). Interestingly, *athb53* × *prAtHB40:GUS* exhibited reduced staining in the root tip as compared with *prAtHB40:GUS* plants, suggesting that AtHB53 is a positive regulator of *AtHB40*. In contrast, AtHB40 did not seem to affect *AtHBB53* expression in roots. Moreover, *AtHB53* was induced by IAA in the root vascular system and columella (Fig. 7c), which raised the possibility that the *AtHB40* induction by auxin was mediated by AtHB53. To test this hypothesis, *prAtHB40:GUS* × *athb53* seedlings were treated with IAA and analyzed by histochemistry (Supplementary Fig. S10). We observed that in *athb53* mutants, *AtHB40* was still expressed in the columella cells but not in the root vasculature. This suggests that the auxin-induced expression of *AtHB40* in the vascular tissue is dependent on AtHB53. In contrast, AtHB40 did not seem to affect *AtHB53* expression in the tip of the primary root because neither *athb40* × *prAtHB53:GUS* nor *prAtHB53:GUS* lines displayed GUS staining.

Altogether, these results indicated that AtHB53 modulates the expression of *AtHB40* both in the vascular system and the root tip, but not vice versa. Both paralogs are regulated by auxin, albeit their action on the targets was not IAA-dependent (Fig. 7d).

4. Discussion

Root gravitropism has been well explained at the beginning of the 20th century by the starch-statolith model stating the sedimentation of

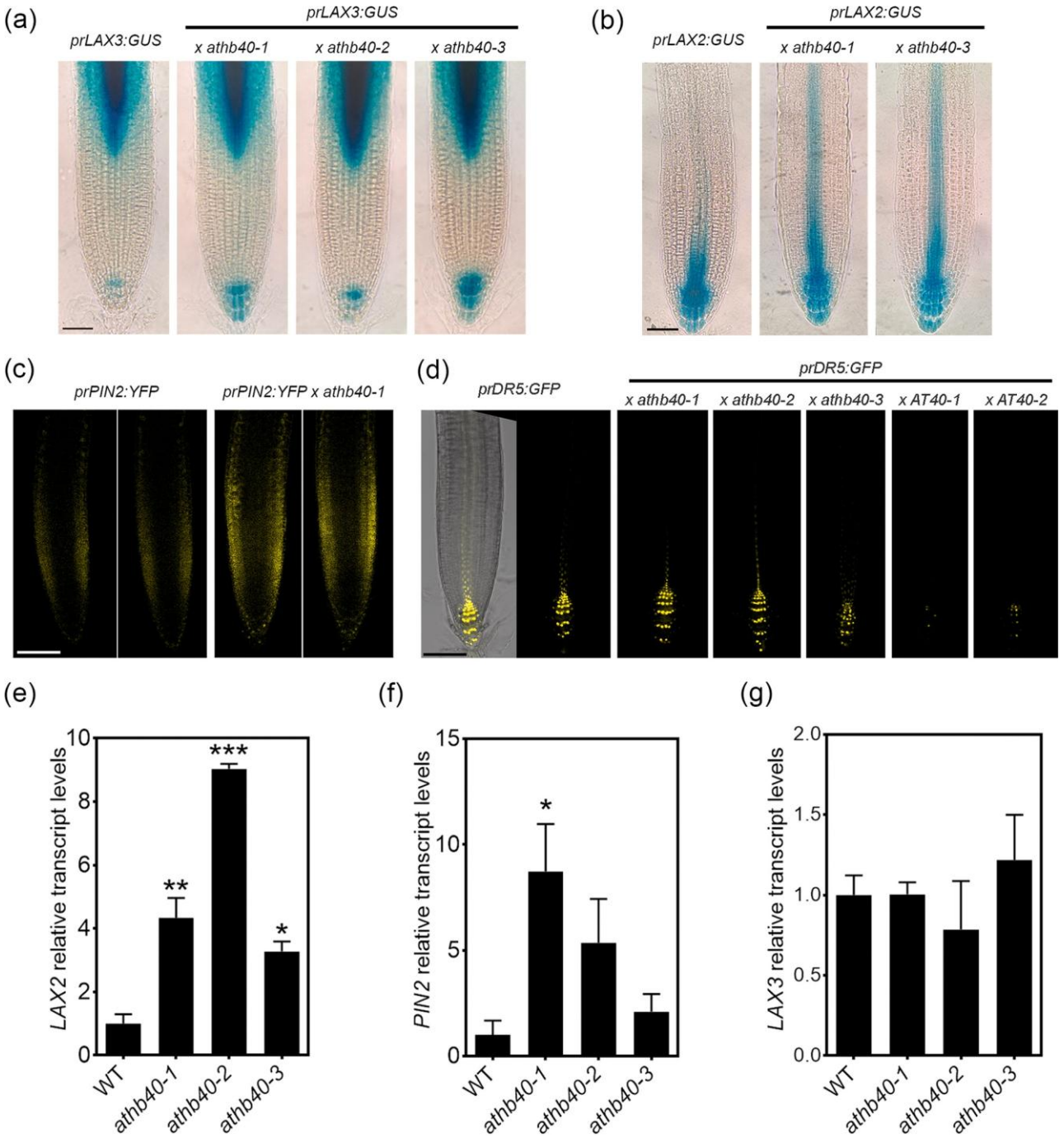

Fig. 5. AtHB40 modulates auxin distribution in the root tip through the regulation of auxin transporter genes. Illustrative pictures of 7-day old *prLAX3:GUS* and *athb40* × *prLAX3:GUS* (*athb40-1, athb40-2,* and *athb40-3*) roots after histochemical staining. (**b**) Illustrative pictures of 7-day-old *prLAX2:GUS* and *athb40* × *prLAX2:GUS* (*athb40-1* and *athb40-3*) roots after histochemical staining. Black bars represent 40 µm. (**c**) Illustrative pictures of 7-day-old *prPIN2:YFP*, and *athb40-1* × *prPIN2:YFP* , visualized by confocal microscopy. The white bar represents 100 µm. (**d**) Illustrative pictures of 7-day-old *DR5:GFP, athb40-1* × *DR5:GFP, athb40-2* × *DR5:GFP, athb40-3* × *DR5:GFP,* AT40-1× *DR5:GFP,* and AT40-2× *DR5:GFP* roots visualized by confocal microscopy. The black bar represents 100 µm. (**e**) Transcript levels of *LAX2* in 7-day-old *athb40* mutant (lines *athb40-1, athb40-2, and athb40-3*) roots compared with the control Col 0 (WT), grown in standard conditions. (**f**) Transcript levels of *PIN2* in 7-day-old *athb40* mutant (lines *athb40-1, athb40-2, and athb40-3*) roots compared with the control Col 0 (WT), grown in standard conditions. (**g**) Transcript levels of *LAX3* in 7-day-old *athb40* mutant (lines *athb40-1, athb40-2, and athb40-3*) roots compared with the control Col 0 (WT), grown in standard conditions. All the values were normalized with the one obtained in Col 0, and represent biological triplicates. Error bars represent SEM. Asterisks indicate significant differences doing an ANOVA test between Col 0 and each transgenic line (** $P < 0.01$, *** $P < 0.001$, **** $P < 0.0001$).

the dense starch-filled amyloplasts (reviewed by Sato et al., 2015). However, there are alternative hypotheses and models, based on changes in the pressure exerted by the cytoplasm on the plasma membrane in response to gravity (Wayne and Staves, 1996), which explain the weak differences in gravitropistic response shown starchless mutants (Kiss and Sack, 1989; Kiss et al., 1996; MacCleery and Kiss, 1999; Fitzelle and Kiss, 2001). Several authors proposed that multiple perception mechanisms might act concomitantly, even outside columella cells (Baldwin et al., 2013).

In this work, we investigated the role of an HD-Zip I TF, AtHB40, in

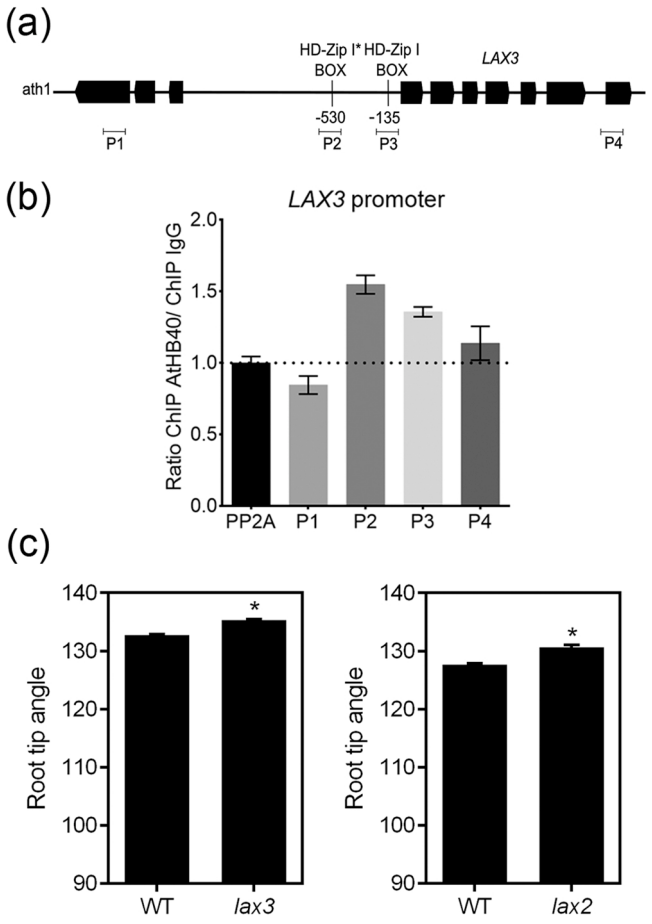

Fig. 6. AtHB40 alters root gravitropism by the regulation of the auxin carriers *LAX2* and *LAX3*; the latter as a direct target. (a) Schematic representation of *LAX3* gene indicating where the designed oligonucleotides match for each one (P1, P2, P3, and P4). PP2A was used as a negative control, determining the background level. **(b)** Chromatin Immunoprecipitation assay (ChIP-PCR) using nuclei obtained from *LexA:minimal35S:HA:HB40* 10-day-old seedlings. Values are expressed as the ratio between *HA* IP and IgG IP used as a negative control. Bars represent SE. (**c**) The angle was measured in *lax3* and *lax2* mutants after the gravitropism assay. Error bars represent SEM. Asterisks indicate significant differences doing a Student's t-test between Col 0 and each transgenic line (* $P < 0.05$).

root development. Expression analyses indicated that it is specifically expressed in columella cells of the primary root. Phenotypic analyses of *AtHB40* loss/gain of function suggest that this gene affects root elongation: *athb40* mutants and overexpressors displayed longer and shorter roots, respectively (Figs. 1, 2). This characteristic is associated with an increment of the cell number in the transition zone (Fig. 2). Besides the altered root length observed in the mutants, the phenotypic evaluation revealed that the *AtHB40* inducible-overexpressors exhibit abnormal response to gravity resulting in a zigzag growth pattern of the root. Furthermore, classic gravitropism assays indicated that AtHB40 is a negative modulator of this response (Fig. 4) because mutants exhibited an enhanced reaction, whereas overexpressors did the opposite. Intriguingly, amyloplasts from *athb40* mutant root tips did not present changes in their morphology or density (Supplementary Fig. S5). However, auxin distribution was significantly altered in *athb40* mutants, as indicated by crosses between them and *DR5:GFP*, *prLAX2:GUS*, *prLAX3:GUS*, and *prPIN2:YFP* plants (Fig. 5).

It has been proposed that the phytohormone auxin acts as the mediating signal between the gravity perception site in the columella where the sedimenting amyloplasts are, and the root elongation zone, where the cell response is finally triggered. Gravitropic stimulated roots from plants transformed with auxin reporters showed differential accumulation of this hormone between the lower and upper side (Ottenschla¨ger et al., 2003; Swarup and Bennett, 2009; Band et al., 2012; Rakusova´ et al., 2015; Vandenbrink and Kiss, 2019). The directional movement of auxin is mediated by auxin carriers, which compose a small family (Bennett et al., 1996). Among them, AUX1 is expressed in the columella and plays an important role in gravitropism; mutants in this gene cannot respond to gravitropic signals. In this work, we showed that *AUX1* expression does not depend on AtHB40 (Supplementary Fig. S7), hinting at alternative pathways controlled by this TF impacting root gravitropism.

Other key actors in root gravitropism are the efflux carriers PIN (PINFORMED), which are asymmetrically localized in the root apex. Auxin asymmetry is initiated by PIN3 and PIN7, whereas AUX1 and PIN2-dependent transport is shootward to the epidermal cells in the elongation zone, through the lateral root cap. PIN2 was found in the lateral root cap, and epidermal and cortical cells, and its asymmetric localization provides directionality to auxin movement (Luschnig et al., 1998; Müller et al., 1998; Friml et al., 2002a, 2002b; Rakusova´ et al., 2015). Notably, auxin concentration is enhanced and directed shootward in *athb40* mutants, and in contrast to *AUX1*, the expression of three auxin carriers (*LAX2*, *LAX3*, and *PIN2*) significantly increased. At the same time, *athb40* mutants exhibited an enhanced gravitropic response, indicating that somehow AtHB40 inhibits such response by, directly or indirectly, repressing the transcription of *LAX2*, *LAX3*, and *PIN2*. It was reported that in adventitious and lateral root formation, the transcriptional module ARF7/ARF19-LBD16/LBD18 plays an important role via the AUX1/LAX3 carriers, albeit indirect (Lee et al., 2015, 2019).

Although neither *LAX2* nor *PIN2* exhibit the cis-regulatory element recognized by HD-Zip I TFs (Palena et al., 1999), their transcript levels in *athb40* mutants, as well as *GUS/YFP* reporters' expression in the crosses *athb40* × *prPIN2:YFP* and *athb40* × *prLAX2:GUS*, were altered, indicating that these genes are indirect targets of AtHB40. On the other hand, *LAX3* was previously reported as a direct target of AtHB40, supported by a Y1H experiment (Porco et al., 2016), and by DAP-Seq analysis (Bartlett et al., 2017). Here, we corroborated the relationship by GUS histochemistry in *athb40* × *prLAX3:GUS* crossed plants and the direct binding by a ChIP assay (Fig. 6). It was suggested that auxin carriers' genes are fine-tuned by an endogenous auxin homeostasis mechanism involving several TFs and other biomolecules (Mellor et al., 2015).

An auxin reflux loop is created by a different localization of PIN2. In the distal elongation zone, this carrier was found on the shootward face, whereas in cortical cells on the rootward, both in epidermal cells (Blilou et al., 2005). Auxin distribution is modulated by many factors composing a complex scenario, including the small secretory peptide GOLVEN, the trafficking modulator TENin1, the phytohormone gibberellin, Ca^{2+}, pH, ROS, nitric oxide, and post-translational modifications, such as (de)phosphorylation (reviewed by Sato et al., 2015). Most of them conduct to PIN2 distribution, pointing to this carrier as the main actor in root gravitropism; however, *pin2* mutants did not show a severe agravitropic phenotype (Blakeslee et al., 2007), indicating that other biomolecules are necessary for this crucial developmental response.

Auxin asymmetry persists up to the point when the root tip angle reaches 40°, which takes approximately 100 min, and then symmetry is restored, and amyloplasts move to the "new bottom" of the cell (Band et al., 2012). Notably, no significant differences between mutant and wild-type plants were observed regarding the morphology and the position of statoliths likely because amyloplasts are not altered by AtHB40, at least in the usually analyzed periods.

Because AtHB40 is one of the three members of the clade VI of HD-Zip I TFs (Arce et al., 2011), which exhibit redundant functions in branching (Gonz´alez-Grandío et al., 2017), we wondered whether they had also redundant functions in roots. The Bar database (Brady et al., 2007; Dinneny et al., 2008; Kilian et al., 2007) indicates that *AtHB53*

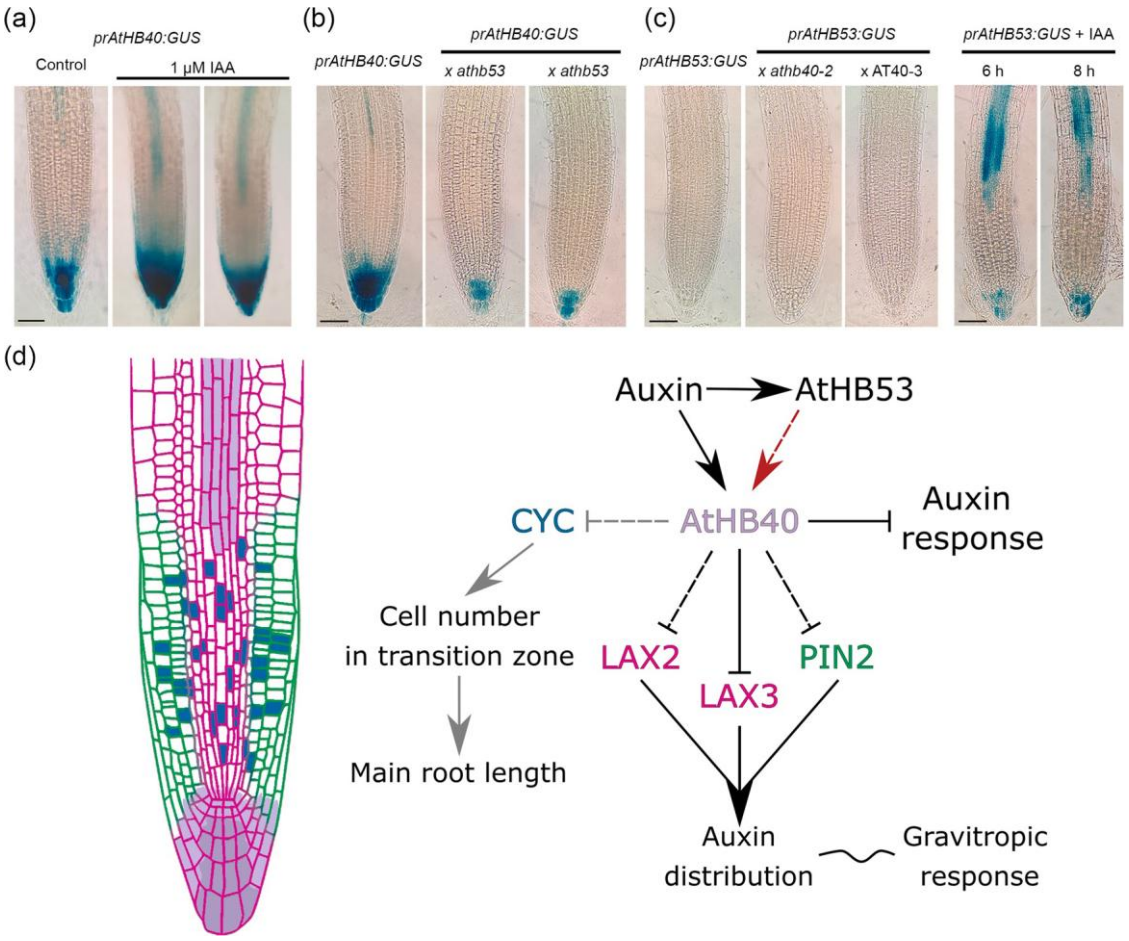

Fig. 7. AtHB53 modulates *AtHB40* expression in the root tip, impacting root growth and the gravitropic response. (**a**) GUS expression in *prAtHB40:GUS* roots treated (right) or not (left) with 1 μM IAA. (**b**) Illustrative pictures of GUS staining in the 7-day-old crosses *athb53* × *prAtHB40:GUS* and (**c**) *athb40* × *prAtHB53:GUS*; *prAtHB53:GUS* before and after induction by IAA. Black bars represent 40 μm. (**d**) Proposed model for the modulation of the gravitropistic response and primary root elongation exerted by AtHB40. Arrows between actors indicate direct regulation. Color codes: lavender indicates *AtHB40* expression; green signals PIN2; magenta shows the overlapped expression of LAX2 and LAX3 and in blue, CYC expression.

was specifically expressed in the procambium and lateral root primordium, whereas *AtHB21* was detected in the xylem pole pericycle, phloem companion, and protophloem, but not in the columella (Perotti et al., 2021a). However, plants transformed with the promoter regions of these paralog genes driving the reporter *GUS* did not show any staining in the root tip (Supplementary Fig. S3), in agreement with the Root Atlas data (Zhang et al., 2019). Another member from this family, AtHB23, was reported as playing a role in root gravitropism. However, AtHB23 action courses via a different mechanism that alters starch turnover and amyloplast formation (Perotti et al., 2022). On the other hand, AtHB52 belonging to clade V (Arce et al., 2011) was involved in ethylene-mediated inhibition of primary root elongation, acting downstream EIN3. Mutants in this gene were insensitive to ethylene whereas overexpressors presented shorter roots. Moreover, AtHB52 regulates the expression of the auxin transport-related genes *PIN2*, *WAVY ROOT GROWTH1* (*WAG1*), and *WAG2* but only the latter in a direct way, suggesting the involvement in crosstalk between auxin and ethylene responses and the need of other intermediate proteins (Miao et al., 2018). The observations done in this work suggest an interplay between AtHB53 and AtHB40 to modulate auxin distribution related to gravitropism (Fig. 7). Further studies will be necessary to elucidate all the relationships established between these genes and the phytohormones.

Summarizing, our data suggest that AtHB40 acts as a repressor in at least two events related to gravitropism (Fig. 7b). Root bending requires cell elongation and division, and AtHB40 emerged as a repressor of *CYCLINB* (Fig. 3). Interestingly, *athb40* mutants exhibited more cells in the transition zone, hinting at a link between AtHB40-mediated repression of cell division and the enhanced gravitropistic response shown by these mutants. This hypothesis is further supported by the opposite phenotype exhibited by *AtHB40* overexpressors.

5. Conclusions

The knowledge of gene transcriptional regulation during gravitropistic sensing and response is very limited so far. Here, we contributed an additional piece to the complex existing scenario. The experimental evidence shown in this work indicates that the HD-Zip I AtHB40 is a repressor of gravitropism by the modulation of auxin distribution through the direct or indirect transcriptional inhibition of the auxin carriers *LAX2*, *LAX3*, and *PIN2* (Fig. 7b). Furthermore, *AtHB40* expression is modulated by auxin-induced AtHB53, which in normal conditions is not expressed in the tip of the primary roots.

CRediT authorship contribution statement

CCM carried out most experiments, FP and CCM carried out amyloplast and ChIP assays, and prepared the figures. PAR participated in the cloning of *prAtHB40$_l$:GUS* and *35S:AtHB40* constructs, and in initial *athb40* root phenotyping. EGG and PC created At40$_{ind}$, *prAtHB40s:GUS*, *prAtHB21:GUS*, and *prAtHB53:GUS* plants. Moreover, they revised, discussed, and helped to improve the MS. RLC conceived, designed, and wrote the manuscript. All the authors carefully revised

and approved the manuscript.

Funding

This work was supported by Agencia Nacional de Promocio´n Científica y Tecnolo´gica, PICT 2017 0305, PICT 2019 01916, and PICT 2020 0805.

CCM, and MFP are currently CONICET Fellows, and PAR was a postdoctoral Fellow until 2018. RLC is a career member of the same institution.

Declaration of Competing Interest

The authors declare that they have no known competing financial interests or personal relationships that could have appeared to influence the work reported in this paper.

Data Availability

Data will be made available on request.

Acknowledgments

We especially thank Dr. Federico Ariel and Dr. Daniel Gonz´alez for helpful discussions and critical reading of the manuscript.

We thank Dr. Ranjan Swarup for kindly providing *lax* mutants as well as *AUX/LAX* promoters fused to *GUS* seeds used in this study to our colleague Javier Moreno.

Appendix A. Supporting information

Supplementary data associated with this article can be found in the online version at doi:10.1016/j.plantsci.2022.111421.

References

A.L. Arce, J. Raineri, M. Capella, J.V. Cabello, R.L. Chan, Uncharacterized conserved motifs outside the HD-Zip domain in HD-Zip subfamily I transcription factors; a potential source of functional diversity, BMC Plant Biol. 11 (2011) 42, https://doi.org/10.1186/1471-2229-11-42.

K. Bainbridge, S. Guyomarc'h, E. Bayer, R. Swarup, M. Bennett, T. Mandel, C. Kuhlemeier, Auxin influx carriers stabilize phyllotactic patterning, Genes Dev. 22 (2008) 810–823, https://doi.org/10.1101/gad.462608.

K.L. Baldwin, A.K. Strohm, P.H. Masson, Gravity sensing and signal transduction in vascular plant primary roots, Am. J. Bot. 100 (2013) 126–142, https://doi.org/10.3732/ajb.1200318.

L.R. Band, D.M. Wells, A. Larrieu, J. Sun, A.M. Middleton, A.P. French, G. Brunoud, E. M. Sato, M.H. Wilson, B. Pe´ret, M. Oliva, R. Swarup, I. Sairanen, G. Parry, K. Ljung, T. Beeckman, J.M. Garibaldi, M. Estelle, M.R. Owen, K. Vissenberg, T.C. Hodgman, T.P. Pridmore, J.R. King, T. Vernoux, M.J. Bennett, Root gravitropism is regulated by a transient lateral auxin gradient controlled by a tipping-point mechanism, Proc. Natl. Acad. Sci. USA 109 (2012) 4668–4673, https://doi.org/10.1073/pnas.1201498109.

A. Bartlett, R.C. O'Malley, S.C. Huang, M. Galli, J.R. Nery, A. Gallavotti, J.R. Ecker, Mapping genome-wide transcription-factor binding sites using DAP-seq, Nat. Protoc. 12 (2017) 1659–1672, https://doi.org/10.1038/nprot.2017.055.

M.J. Bennett, A. Marchant, H.G. Green, S.T. May, S.P. Ward, P.A. Millner, A.R. Walker, B. Schulz, K.A. Feldmann, Arabidopsis AUX1 gene: a permease-like regulator of root gravitropism, Science 273 (1996) 948–950, https://doi.org/10.1126/science.273.5277.948.

J.J. Blakeslee, A. Bandyopadhyay, O.R. Lee, J. Mravec, B. Titapiwatanakun, M. Sauer, S. N. Makam, Y. Cheng, R. Bouchard, J. Adamec, M. Geisler, A. Nagashima, T. Sakai, E. Martinoia, J. Friml, W.A. Peer, A.S. Murphy, Interactions among PIN-FORMED and P-glycoprotein auxin transporters in Arabidopsis, Plant Cell 19 (2007) 131–147, https://doi.org/10.1105/tpc.106.040782.

I. Blilou, J. Xu, M. Wildwater, V. Willemsen, I. Paponov, J. Friml, R. Heidstra, M. Aida, K. Palme, B. Scheres, The PIN auxin efflux facilitator network controls growth and patterning in Arabidopsis roots, Nature 433 (2005) 39–44, https://doi.org/10.1038/nature03184.

S.M. Brady, D.A. Orlando, J.Y. Lee, J.Y. Wang, J. Koch, J.R. Dinneny, D. Mace, U. Ohler, P.N. Benfey, A high-resolution root spatiotemporal map reveals dominant expression patterns, Science 318 (2007) 801–806, https://doi.org/10.1126/science.1146265.

M. Capella, P.A. Ribone, A.L. Arce, R.L. Chan, Homeodomain-leucine zipper transcription factors: structural features of these proteins, unique to plants, in: D. H. Gonz´alez (Ed.), Plant Transcription Factors: Evolutionary, Structural and Functional Aspects, 2016, pp. 113–126, https://doi.org/10.1016/B978-0-12-800854-6.00007-5.

S.J. Clough, A.F. Bent, Floral dip: a simplified method for Agrobacterium-mediated transformation of Arabidopsis thaliana, Plant J. 16 (1998) 735–743, https://doi.org/10.1046/j.1365-313x.1998.00343.x.

J.R. Dinneny, T.A. Long, J.Y. Wang, J.W. Jung, D. Mace, S. Pointer, C. Barron, S. M. Brady, J. Schiefelbein, P.N. Benfey, Cell identity mediates the response of Arabidopsis roots to abiotic stress, Science 320 (2008) 942–945, https://doi.org/10.1126/science.1153795.

S. Dong, D. Tarkowska, M. Sedaghatmehr, M. Molochko, S. Gupta, B. Mueller-Roeber, S. Balazadeh, The HB40-JUB1 transcriptional regulatory network controls gibberellin homeostasis in Arabidopsis, Mol. Plant 15 (2022) 322–339, https://doi.org/10.1016/j.molp.2021.10.007.

K.J. Fitzelle, J.Z. Kiss, Restoration of gravitropic sensitivity in starch deficient mutants of Arabidopsis by hypergravity, J. Exp. Bot. 52 (2001) 265–275, https://doi.org/10.1093/jxb/52.355.265.

J. Friml, E. Benkov´a, I. Blilou, J. Wisniewska, T. Hamann, K. Ljung, S. Woody, G. Sandberg, B. Scheres, G. Jürgens, K. Palme, AtPIN4 mediates sink-driven auxin gradients and root patterning in Arabidopsis, Cell 108 (2002a) 661–673, https://doi.org/10.1016/s0092-8674(02)00656-6.

J. Friml, J. Wisniewska, E. Benkova, K. Mendgen, K. Palme, Lateral relocation of auxin efflux regulator PIN3 mediates tropism in Arabidopsis, Nature 415 (2002b) 806–809, https://doi.org/10.1038/415806a.

D.H. Gonzalez, Introduction to transcription factor structure and function, in: Plant Transcription Factors: Evolutionary, Structural and Functional Aspects, Elsevier ed., 2016, pp. 3–11.

E. Gonz´alez-Grandío, A. Pajoro, J.M. Franco-Zorrilla, C. Taranco´n, R.G. Immink, P. Cubas, Abscisic acid signaling is controlled by a BRANCHED1/HD-ZIP I cascade in Arabidopsis axillary buds, Proc. Natl. Acad. Sci. U.S.A. 114 (2) (2017) E245–E254, https://doi.org/10.1073/pnas.1613199114.

E. Henriksson, A.S. Olsson, H. Johannesson, H. Johansson, J. Hanson, P. Engstro¨m, E. So¨derman, Homeodomain leucine zipper class I genes in Arabidopsis. Expression patterns and phylogenetic relationships, Plant Physiol. 139 (2005) 509–518, https://doi.org/10.1104/pp.105.063461.

R.A. Jefferson, T.A. Kavanagh, M.W. Bevan, GUS fusions: beta-glucuronidase as a sensitive and versatile gene fusion marker in higher plants, EMBO J. 6 (1987) 3901–3907, https://doi.org/10.1002/j.1460-2075.1987.tb02730.x.

H. Johannesson, Y. Wang, P. Engstro¨m, DNA-binding and dimerization preferences of Arabidopsis homeodomain–leucine zipper transcription factors in vitro, Plant Mol. Biol. 45 (2001) 63–73, https://doi.org/10.1023/a:1006423324025.

J. Kilian, D. Whitehead, J. Horak, D. Wanke, S. Weinl, O. Batistic, C. D'Angelo, E. Bornberg-Bauer, J. Kudla, K. Harter, The AtGenExpress global stress expression data set: protocols, evaluation and model data analysis of UV-B light, drought and cold stress responses, Plant J. 50 (2007) 347–363, https://doi.org/10.1111/j.1365-313X.2007.03052.x.

J.Z. Kiss, F.D. Sack, Reduced gravitropic sensitivity in roots of a starch-deficient mutant of Nicotiana sylvestris, Planta 180 (1989) 123–130, https://doi.org/10.1007/BF02411418.

J.Z. Kiss, J.B. Wright, T. Caspar, Gravitropism in roots of intermediate-starch mutants of Arabidopsis, Physiol. Plant. 97 (1996) 237–244, https://doi.org/10.1034/j.1399-3054.1996.970205.x.

H.W. Lee, C. Cho, J. Kim, Lateral organ boundaries domain16 and 18 act downstream of the AUXIN1 and LIKE-AUXIN3 auxin influx carriers to control lateral root development in Arabidopsis, Plant Physiol. 168 (4) (2015) 1792–1806, https://doi.org/10.1104/pp.15.00578.

H.W. Lee, C. Cho, S.K. Pandey, Y. Park, M.J. Kim, J. Kim, LBD16 and LBD18 acting downstream of ARF7 and ARF19 are involved in adventitious root formation in Arabidopsis, BMC Plant Biol. 19 (1) (2019) 46, https://doi.org/10.1186/s12870-019-1659-4.

Y. Liu, J. Xu, S. Guo, S. Zhao, H. Tian, S. Dai, X. Kong, Z. Ding, AtHB7/12 regulate root growth in response to aluminum stress, Int. J. Mol. Sci. 21 (2020) 4080, https://doi.org/10.3390/ijms21114080.

L.E. Lucero, P.A. Manavella, D.E. Gras, F.D. Ariel, D.H. Gonzalez, Class I and Class II TCP transcription factors modulate SOC1-dependent flowering at multiple levels, Mol. Plant 10 (2017) 1571–1574, https://doi.org/10.1016/j.molp.2017.09.001.

C. Luschnig, R.A. Gaxiola, P. Grisafi, G.R. Fink, EIR1, a root specific protein involved in auxin transport, is required for gravitropism in Arabidopsis thaliana, Genes Dev. 12 (1998) 2175–2187, https://doi.org/10.1101/gad.12.14.2175.

S.A. MacCleery, J.Z. Kiss, Plastid sedimentation kinetics in roots of wild-type and starch-deficient mutants of Arabidopsis, Plant Physiol. 120 (1999) 183–192, https://doi.org/10.1104/pp.120.1.183.

A. Marchant, R. Bhalerao, I. Casimiro, J. Eklo¨f, P.J. Casero, M. Bennett, G. Sandberg, AUX1 promotes lateral root formation by facilitating indole-3-acetic acid distribution between sink and source tissues in the Arabidopsis seedling, Plant Cell 14 (2002) 589–597, https://doi.org/10.1105/tpc.010354.

A. Marchant, J. Kargul, S.T. May, P. Muller, A. Delbarre, C. Perrot-Rechenmann, M. J. Bennett, AUX1 regulates root gravitropism in Arabidopsis by facilitating auxin uptake within root apical tissues, EMBO J. 18 (1999) 2066–2073, https://doi.org/10.1105/tpc.010354.

N. Mellor, B. P´eret, S. Porco, I. Sairanen, K. Ljung, M. Bennett, J. King, Modelling of Arabidopsis LAX3 expression suggests auxin homeostasis, J. Theor. Biol. 366 (2015) 57–70, https://doi.org/10.1016/j.jtbi.2014.11.003.

Z.Q. Miao, P.X. Zhao, J.L. Mao, L.-H. Yu, Y. Yuan, H. Tang, Z.-B. Liu, C.-B. Xiang, HOMEOBOX PROTEIN52 mediates the crosstalk between ethylene and auxin signaling during primary root elongation by modulating auxin transport-related gene expression, Plant Cell 30 (2018) 2761–2778, https://doi.org/10.1105/tpc.18.00584.

H. Motte, S. Vanneste, T. Beeckman, Molecular and environmental regulation of root development, Annu. Rev. Plant Biol. 70 (2019) 465–488, https://doi.org/10.1146/annurev-arplant-050718-100423.
A. Müller, C. Guan, L. G¨alweiler, P. T¨anzler, P. Huijser, A. Marchant, G. Parry, M. Bennett, E. Wisman, K. Palme, AtPIN2 defines a locus of Arabidopsis for root gravitropism control, EMBO J. 17 (1998) 6903–6911, https://doi.org/10.1093/emboj/17.23.6903.
L. Muller, M.J. Bennett, A. French, D.M. Wells, R. Swarup, Root gravitropism: quantification, challenges, and solutions, Methods Mol. Biol. 1761 (2018) 103–112, https://doi.org/10.1007/978-1-4939-7747-5_8.
M. Nakayama, Y. Kaneko, Y. Miyazawa, N. Fujii, N. Higashitani, S. Wada, H. Ishida, K. Yoshimoto, K. Shirasu, K. Yamada, M. Nishimura, H. Takahashi, A possible involvement of autophagy in amyloplast degradation in columella cells during hydrotropic response of Arabidopsis roots, Planta 236 (2012) 999–1012, https://doi.org/10.1007/s00425-012-1655-5.
I. Ottenschla¨ger, P. Wolff, C. Wolverton, R.P. Bhalerao, G. Sandberg, H. Ishikawa, M. Evans, K. Palme, Gravity-regulated differential auxin transport from columella to lateral root cap cells, Proc. Natl. Acad. Sci. USA 100 (2003) 2987–2991, https://doi.org/10.1073/pnas.0437936100.
C.M. Palena, D.H. Gonzalez, R.L. Chan, A monomer–dimer equilibrium modulates the interaction of the sunflower homeodomain–leucine zipper protein HAHB-4 with DNA, Biochem. J. 341 (1999) 81–87, https://doi.org/10.1042/0264-6021:3410081.
M.F. Perotti, A.L. Arce, F.D. Ariel, C.M. Figueroa, R.L. Chan, The transcription factor AtHB23 modulates starch turnover for root development and plant survival under salinity, Environ. Exp. Bot. 201 (2022), 104994, https://doi.org/10.1016/j.envexpbot.2022.104994.
M.F. Perotti, A.L. Arce, R.L. Chan, The underground life of homeodomain-leucine zipper transcription factors, J. Exp. Bot. 72 (2021) 4005–4021, https://doi.org/10.1093/jxb/erab112.
M.F. Perotti, F.D. Ariel, R.L. Chan, Lateral root development differs between main and secondary roots and depends on the ecotype, Plant Signal. Behav. 15 (2020), 1755504, https://doi.org/10.1080/15592324.2020.1755504.
M.F. Perotti, P.A. Ribone, J.V. Cabello, F.D. Ariel, R.L. Chan, AtHB23 participates in the gene regulatory network controlling root branching, and reveals differences between secondary and tertiary roots, Plant J. 100 (2019) 1224–1236, https://doi.org/10.1111/tpj.14511.
S. Porco, A. Larrieu, Y. Du, A. Gaudinier, T. Goh, K. Swarup, R. Swarup, B. Kuempers, A. Bishopp, J. Lavenus, I. Casimiro, K. Hill, E. Benkova, H. Fukaki, S.M. Brady, B. Scheres, B. P´eret, M.J. Bennett, Lateral root emergence in Arabidopsis is dependent on transcription factor LBD29 regulation of auxin influx carrier LAX3, Development 143 (2016) 3340–3349, https://doi.org/10.1242/dev.136283.
H. Rakusov´a, M. Fendrych, J. Friml, Intracellular trafficking and PIN-mediated cell polarity during tropic responses in plants, Curr. Opin. Plant Biol. 23 (2015) 116–123, https://doi.org/10.1016/j.pbi.2014.12.002.
P.A. Ribone, M. Capella, R.L. Chan, Functional characterization of the homeodomain leucine zipper I transcription factor AtHB13 reveals a crucial role in Arabidopsis, Dev. J. Exp. Bot. 66 (2015) 5929–5943, https://doi.org/10.1093/jxb/erv302.
E.M. Sato, H. Hijazi, M.J. Bennett, K. Vissenberg, R. Swarup, New insights into root gravitropic signalling, J. Exp. Bot. 66 (2015) 2155–2165, https://doi.org/10.1093/jxb/eru515.
A.T. Silva, P.A. Ribone, R.L. Chan, W. Ligterink, H.W.M. Hilhorst, A predictive co-expression network identifies novel genes controlling the seed-to-seedling phase transition in Arabidopsis thaliana, Plant Physiol. 170 (2016) 2218–2231, https://doi.org/10.1104/pp.15.01704.
O. Son, H.Y. Cho, M.R. Kim, H. Lee, M.S. Lee, E. Song, J.H. Park, K.H. Nam, J.Y. Chun, H. J. Kim, S.K. Hong, Y.Y. Chung, C.G. Hur, H.T. Cho, C.I. Cheon, Induction of a homeodomain-leucine zipper gene by auxin is inhibited by cytokinin in Arabidopsis roots, Biochem. Biophys. Res. Commun. 326 (2005) 203–209, https://doi.org/10.1016/j.bbrc.2004.11.014.
S.-H. Su, N. Gibbs, A. Jancewicz, P. Masson, Molecular mechanisms of root gravitropism, Curr. Biol. 27 (2017) R964–R972, https://doi.org/10.1016/j.cub.2017.07.015.
S.-H. Su, P. Masson, A new wrinkle in our understanding of the role played by auxin in root gravitropism, New Phytol. 224 (2019) 543–546, https://doi.org/10.1111/nph.16140.
R. Swarup, M.J. Bennett, Root gravitropism, Annu. Plant Rev. 37 (2009) 157–174, https://doi.org/10.1002/9781119312994.apr0401.
K. Swarup, E. Benkov´a, R. Swarup, I. Casimiro, B. Pe´ret, Y. Yang, G. Parry, E. Nielsen, I. De Smet, S. Vanneste, M.P. Levesque, D. Carrier, N. James, V. Calvo, K. Ljung, E. Kramer, R. Roberts, N. Graham, S. Marillonnet, K. Patel, J.D. Jones, C.G. Taylor, D.P. Schachtman, S. May, G. Sandberg, P. Benfey, J. Friml, I. Kerr, T. Beeckman, L. Laplaze, M.J. Bennett, The auxin influx carrier LAX3 promotes lateral root emergence, Nat. Cell Biol. 10 (2008) 946–954, https://doi.org/10.1038/ncb1754.
J.P. Vandenbrink, J.Z. Kiss, Plant responses to gravity, Semin. Cell Dev. Biol. 92 (2019) 122–125, https://doi.org/10.1016/j.semcdb.2019.03.011.
R. Wayne, M.P. Staves, A down to earth model of gravisensing or Newton's Law of Gravitation from the apple's perspective, Physiol. Plant. 98 (1996) 917–921, https://doi.org/10.1111/j.1399-3054.1996.tb06703.x.
B. Wicke, E. Smeets, V. Dornburg, B. Vashev, T. Gaiser, W. Turkenburg, A. Faaij, The global technical and economic potential of bioenergy from salt-affected soils, Energy Environ. Sci. 4 (2011) 2669, https://doi.org/10.1039/C1EE01029H.
L. Zhang, P. Wu, W. Li, T. Feng, J. Shockey, L. Chen, L. Zhang, S. Lü, Triacylglycerol biosynthesis in shaded seeds of tung tree (Vernicia fordii) is regulated in part by Homeodomain Leucine Zipper 21, Plant J. 108 (2021) 1735–1753, https://doi.org/10.1111/tpj.15540.
T.Q. Zhang, Z.G. Xu, G.D. Shang, J.W. Wang, A single-cell RNA sequencing profiles the developmental landscape of arabidopsis root, Mol. Plant 12 (2019) 648–660, https://doi.org/10.1016/j.molp.2019.04.004.